Supplemental Material

Chatterjee and Banoth et al., 2016

Description of variance-based global sensitivity analysis

We have implemented a variance-based global sensitivity analysis to determine the kinetic parameters that play a critical role in signaling crosstalk. We randomly and simultaneously varied a select set of kinetic parameters within a pre-defined range (± 25% of the nominal value) with iterative quasi-Monte Carlo sampling. We had earlier defined the crosstalk index as the ratio of total RelA nuclear activity induced in a 24-hour time period upon costimulation to the sum of the RelA nuclear activities induced by individual stimuli (Fig. 2C). We quantified the contribution of the uncertainty in each individual group of input parameters to the uncertainty of the model output (the crosstalk index) by estimating total effect indexes and standardized regression coefficients as described below.

First, we assumed that $Y = f(\mathbf{X})$ represents a nonlinear mathematical relationship that has been computationally modeled, where Y is the model output and $\mathbf{X}$ is the array of inputs. The variance decomposition scheme described earlier, suggests (*46*):

$$V(Y) = \sum_i V_i + \sum_i \sum_{j>i} V_{ij} + \cdots + V_{12\ldots k} \qquad \text{(Eq. 1)}$$

where $V(Y)$ indicates the total unconditional variance and V_i (also known as the "first order effect") reflects the partial variance of the model output when the i^{th} parameter (i = 1, 2, … k) is fixed for a set of simulations. Succeeding terms in the equation represent partial variances when more than one parameter is fixed while changing the others using Monte Carlo sampling. As described previously (*21*), a first-order partial variance term V_i can be written as:

$$V_i = V_{X_i}\left[E_{\mathbf{X}_{\sim i}}(Y|X_i)\right] \qquad \text{(Eq. 2)}$$

Here, $\mathbf{X}$ indicates an $N \times k$ matrix, where k is the total number of parameter groups being simultaneously perturbed and N is the total number of model simulations or the sample size. For any simulation chosen from N, X_i depicts a generic parameter. In the expression $(Y|X_i)$, Y indicates the scalar model output when X_i is the input for simulations. The expectation $E_{\mathbf{X}_{\sim i}}(Y|X_i)$ in Eq. 2 is computed using the $N \times (k-1)$ matrix, denoted as $\mathbf{X}_{\sim i}$, which excludes the i^{th} column while X_i is held constant during the simulations. The variance in the expected values $E_{\mathbf{X}_{\sim i}}(Y|X_i)$ obtained for simulations carried out for all values of X_i is given by $V_{X_i}[E_{\mathbf{X}_{\sim i}}(Y|X_i)]$. Accordingly, the first-order sensitivity index for the i^{th} parameter (S_i) is defined as:

$$S_i = \frac{V_{X_i}\left[E_{\mathbf{X}_{\sim i}}(Y|X_i)\right]}{V(Y)} \qquad \text{(Eq. 3)}$$

However, the first-order sensitivity index does not account for higher-order interactions. To circumvent this problem, the total effect index was derived as a variance-based index (*47*) that collectively estimates the first-order and all other higher-order influences of a given parameter or a group of parameters on the model output. The total effect index is described as follows:

$$S_{Ti} = \frac{E_{\mathbf{X}_{\sim i}}\left[V_{X_i}(Y|\mathbf{X}_{\sim i})\right]}{V(Y)} = 1 - \frac{V_{\mathbf{X}_{\sim i}}\left[E_{X_i}(Y|\mathbf{X}_{\sim i})\right]}{V(Y)} \qquad \text{(Eq. 4)}$$

As such, the total effect index (S_{Ti}) is better suited for multiparametric analyses to identify sensitive and insensitive parameters unambiguously. The total effect index of the i^{th} parameter is a measure of the residual of the first-order effect of $\mathbf{X}_{\sim i}$ subtracted from the total unconditional variance $V(Y)$.

Here, we used the Sobol quasi-random sequences for selected parameter values (Fig. 2B and table S1) for Monte Carlo sampling (*46*). Notably, it was shown that quasi-random, low-discrepancy sequences, such as the Sobol sequence, exhibit superior convergence properties compared to pseudo-random number generators (*21*). We used the algorithm described below (*21*) to calculate the total effect index of the i^{th} parameter as follows:

$$E_{\mathbf{X}_{\sim i}}\left[V_{X_i}(Y|\mathbf{X}_{\sim i})\right] = \frac{1}{2N}\sum_{J=1}^{N}\left\{f(\mathbf{A})_J - f(\mathbf{A}_{\mathbf{B}}^{(i)})_J\right\}^2 \quad \text{(Eq. 5)}$$

A and **B** represent differently sampled (quasi-random) matrices, where each column (i) consists of various values of a given kinetic parameter within the predefined range. The matrix $\mathbf{A}_{\mathbf{B}}^{(i)}$ is generated by the substitution of the i^{th} column of **A** with the i^{th} column of **B**. The J^{th} row (J = 1, 2, … , N) of the matrices $(\mathbf{A})_J$ and $(\mathbf{A}_{\mathbf{B}}^{(i)})_J$ was used iteratively in the quasi Monte Carlo simulations.

Adhering to Saltelli et. al. (*21*), we chose a more efficient radial sampling strategy for this algorithm. A standard bootstrapping technique was used to calculate the error range of the total effect indexes to avoid possible bias in the data. Error ranges of the bootstrapping were as follows: GR-6: ± 0.0003351; GR-7: ± 0.0000042; GR-8: ± 0.0000049; GR-9: ± 0.0004891; GR-15: ± 0.0001252; GR-16: ± 0.0000055; GR-17: ± 0.0000051; GR-18: ± 0.0003309; GR-19: ± 0.0001258; GR-37: ± 0.0001248; GR-38: ± 0.0000039; GR-39: ± 0.0000010; GR-40: ± 0.0000092; and GR-41: ± 0.0000441. The convergence of the total effect index S_{Ti} was verified through $N \times (k+1)$ number of simulations, where N was varied from 10 to 1000 for k = 14 parameter groups (see fig. S3A). Our analysis revealed that the total effect index for different parameter groups ceases to fluctuate when the sample number is sufficiently high. We showed the result for N = 1000 simulations (Fig. 2D).

Finally, we calculated standardized regression coefficients using these randomly sampled values for a given parameter group as independent variables and crosstalk index output as the dependent variable (fig. S3B) (*48*). Sample parameters and crosstalk outputs were scaled to their respective standard deviations. Regression coefficients of these standardized data were calculated by least square methods and plotted (Fig. 2E). A two-tailed student's t test confirmed a statistically significant deviation from the null value for the parameter groups GR-6, GR-9, GR-15, GR-18, GR-19, and GR-37 (Fig. 2E). A residual plot derived from our regression analyses (fig. S3C) revealed randomly scattered, standardized errors were distributed uniformly about the independent variable axis.

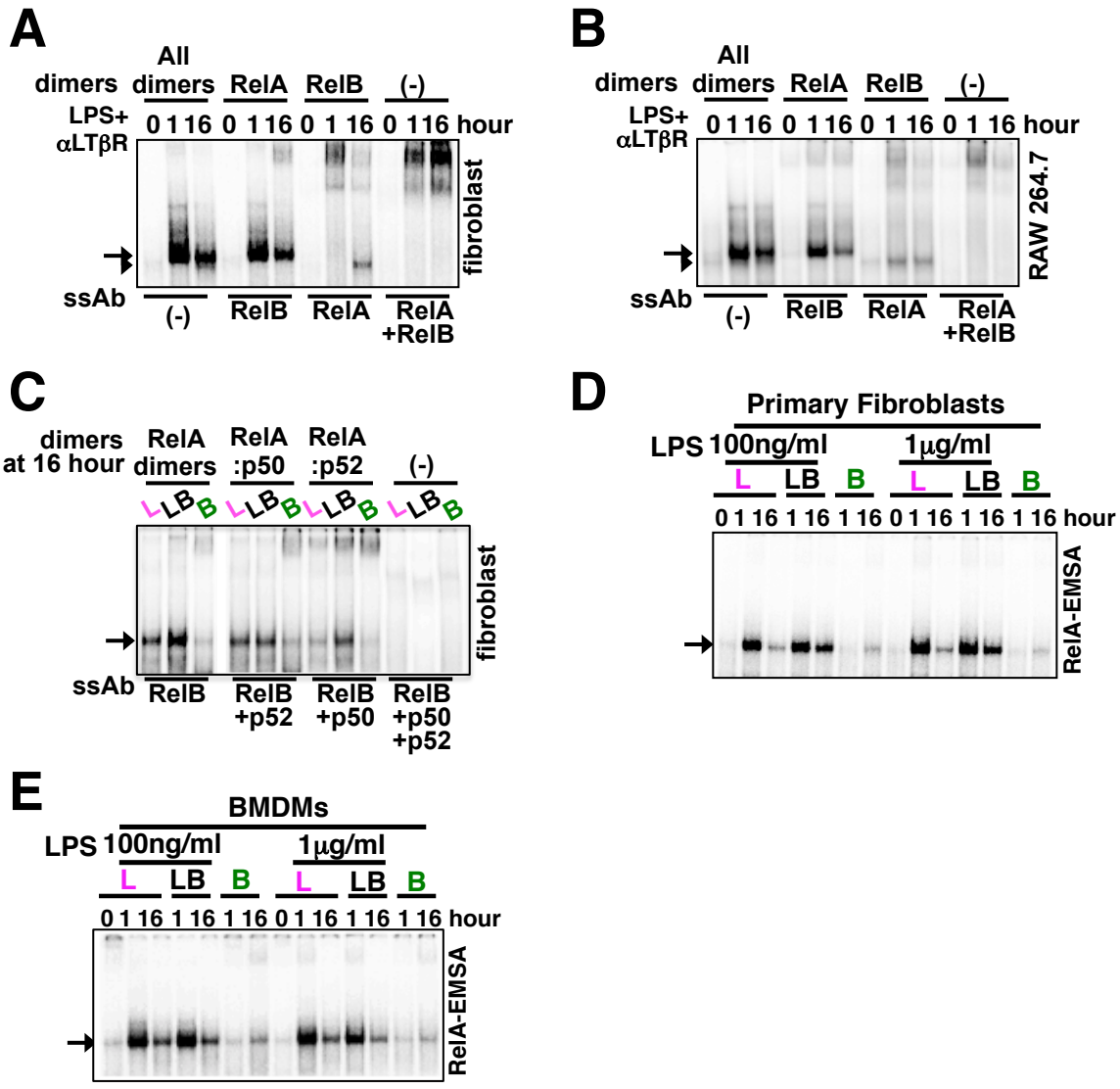

Fig. S1. NF-κB signaling in fibroblasts and macrophages. (**A** and **B**) Immortalized mouse embryonic fibroblasts (MEFs) (A) and RAW 264.7 macrophage cells (B) were stimulated for the indicated times with LPS and αLTβR before being subjected to EMSA and supershift analyses of the DNA-binding activity of NF-κB. The arrow and arrowhead indicate RelA and RelB DNA binding complexes, respectively. Nuclear DNA binding activity of RelA was revealed by supershifting RelB with an anti-RelB antibody. Similarly, DNA binding activity of RelB was unmasked by supershifting RelA. Data are representative of three experiments. (**C**) Supershift analysis with antibodies against the indicated NF-κB subunits were performed to examine RelA activity induced in fibroblasts 16 hours after they were stimulated with LPS (L), αLTβR (B), or both (LB). Data are representative of three experiments. (**D**) Primary MEFs were stimulated for the indicated times with LPS alone (at either of the two indicated concentrations), αLTβR (0.3 μg/ml), or both before being subjected to RelA-EMSA analysis. Data are representative of three experiments. (**E**) Primary bone marrow–derived macrophages (BMDMs) were stimulated with LPS alone (at either of the two indicated concentrations), αLTβR (0.3 μg/ml), or both before being subjected to RelA-EMSA analysis. Data are representative of three experiments.

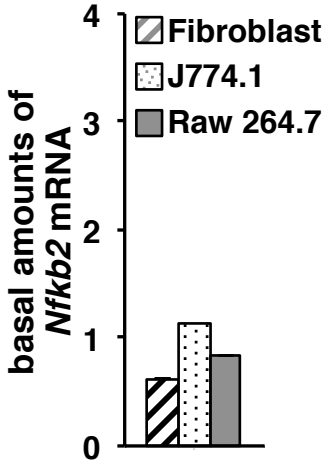

Fig. S2. Constitutive expression of *Nfkb2* in various cell lines. Fibroblasts, J774.1 cells, and RAW 264.7 cells were subjected to quantitative RT-PCR analysis of the basal amount of *Nfkb2* mRNA normalized to that of *Actb* mRNA. Data are representative of three experiments.

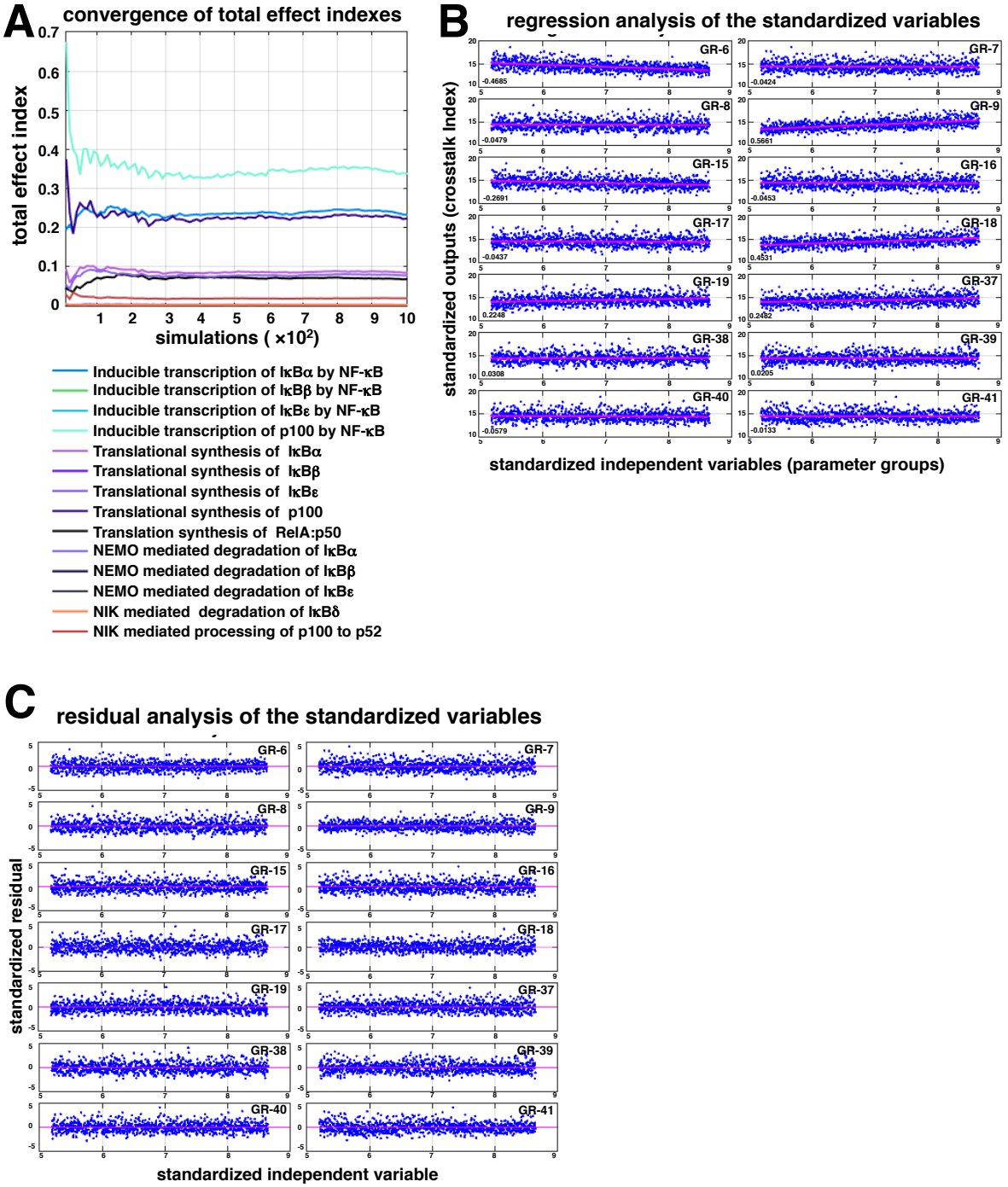

Fig. S3. Variance-based global sensitivity analysis of NF-κB system model v. 1.0. (**A**) Examination of the convergence of total effect indexes for the individual parameter groups presented in Fig. 2D. (**B**) Regression analysis of the standardized variables. The parameter group numbers used as independent variables are shown in the top right corner of each plot. Standardized regression coefficient values are depicted in the bottom left corner of each plot. (**C**) Residual plots for standardized regression analysis reveal that the residuals are distributed evenly on both sides of the regression curves (magenta line) for these plots. These results ascertain that there is no noticeable nonlinearity in the dependent variables and that linear regression is appropriate.

A

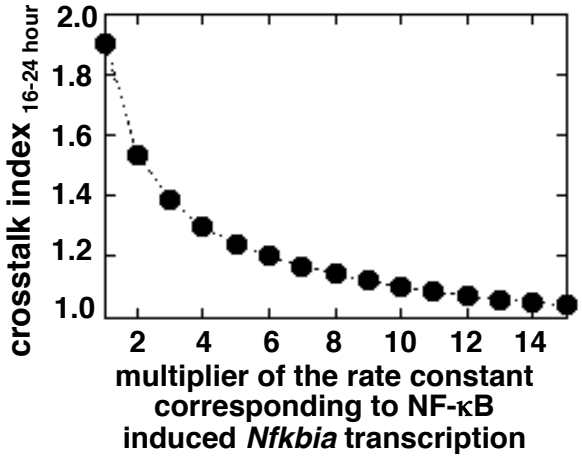

B

five-κB promoter:

CACATTCCACAGCTGGATCCAAGCTAG**GGGACTTTCC**GCTTG**GGGACTTTCC**GCT
G**GGGACTTTCC**GCTG**GGGACTTTCC**GCTG**GGGACTTTCC**GCGGTGACTCTAGAGG
G**TATATA**ATGGAAGCTCGAATTCCAGCTTGGCATTCCGGTACTGTTGGTAAA**ATG**

one-κB promoter:

CACATTCCACAGCTGGATCCAAGCTAG**TCTACTTTCC**GCTTG**TCTACTTTCC**GCT
G**TCTACTTTCC**GCTG**GGGACTTTCC**GCTG**TCTACTTTCC**GCGGTGACTCTAGAGG
G**TATATA**ATGGAAGCTCGAATTCCAGCTTGGCATTCCGGTACTGTTGGTAAA**ATG**

Fig. S4. The enhanced rate of RelA-responsive IκBα synthesis is inversely correlated with pathway crosstalk. (**A**) Graph showing the crosstalk index as a function of the rate constant corresponding to the RelA-induced synthesis of *Nfkbia* mRNA. The crosstalk index was computed from the activity of nuclear RelA induced between 16 and 24 hours of model simulations. (**B**) DNA sequences corresponding to the five-κB–containing promoter and the one-κB–containing promoter that were used in this study to produce IκBα in *Nfkbia*$^{-/-}$ fibroblasts. The κB elements are indicated in blue, whereas the mutated κB elements are indicated in magenta. The TATA box and the start codon are shown in green.

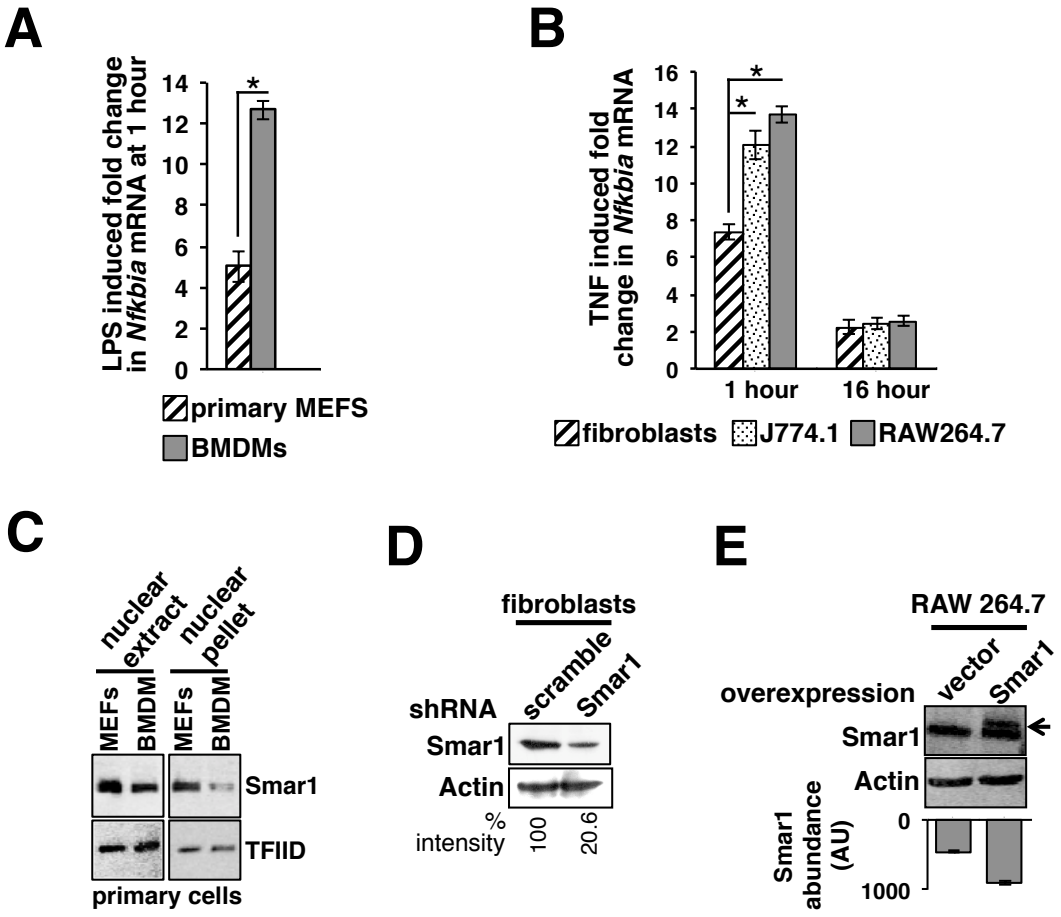

Fig. S5. Smar1 inhibits RelA-induced *Nfkbia* expression during LPS signaling. (**A**) Primary MEFs and BMDMs were treated for 1 hour with LPS before being subjected to quantitative RT-PCR analysis of *Nfkbia* mRNA abundance normalized to that of *Actb* mRNA. Data are means ± SEM of three independent experiments. **P* < 0.05 by two-tailed student's *t* test. (**B**) Immortalized fibroblasts, J774.1 cells, and RAW 264.7 cells were treated with TNF for the indicated times before being subjected to quantitative RT-PCR analysis of *Nfkbia* mRNA abundance normalized to that of *Actb* mRNA. Data are means ± SEM of three independent experiments. **P* < 0.01. (**C**) Primary MEFs and BMDMs were fractionated to generate nuclear extracts and nuclear pellets, which were then analyzed by Western blotting with antibodies against the indicated proteins. TFIID served as a loading control. Western blots are representative of two experiments. (**D**) Immortalized wild type fibroblasts transduced with retrovirus particles expressing either a scrambled shRNA or a Smar1-specific shRNA were subjected to Western blotting analysis with antibodies against the indicated proteins. Residual amount of Smar1 upon knockdown was quantified and presented as % of control cells. (**E**) RAW 264.7 cells were transfected with either p3XFLAG-CMV or p3XFLAG-CMV-Smar1. Forty hours later, the cells were analyzed by Western blotting with antibodies against the indicated proteins. The arrow indicates FLAG-tagged Smar1. Relative amounts of Smar1 protein was quantified and indicated at the bottom of the immunoblot. Data are means ± SEM of three independent experiments.

Table S1. List of parameter groups and kinetic rate constants.

Parameter # (k_n)	Reaction	Parameter value/rate constant	Parameter grouping (group identity)	Justification for parameter grouping and inclusion or exclusion for perturbation
1	➔tIkBa	6.20E-02 $nM.min^{-1}$	signal independent constitutive synthesis of mRNA encoding IκBα **(GR-1)**	**excluded**; core promoter architecture, which is invariant in different cell-types, largely determines the rate of constitutive mRNA synthesis. Accordingly, rate constant related to constitutive synthesis of *Nfkbia* mRNA encoding IκBα were excluded from the sensitivity analyses.
2	➔tIkBb	2.00E-03 $nM.min^{-1}$	signal independent constitutive synthesis of mRNA encoding IκBβ **(GR-2)**	**excluded**; Justification for exclusion is similar to GR-1.
3	➔tIkBe	2.50E-04 $nM.min^{-1}$	signal independent constitutive synthesis of mRNA encoding IκBε **(GR-3)**	**excluded**; Justification for exclusion is similar to GR-1.
4	➔tp100	1.90E-04 $nM.min^{-1}$	signal independent constitutive synthesis of mRNA encoding p100/*Nfkb2* **(GR-4)**	**excluded**; Justification for exclusion is similar to GR-1.
5	➔tNFkB1 (NFkB1 represents RelA:p50 dimer)	1.40E-05 $nM.min^{-1}$	signal independent constitutive synthesis of mRNA encoding composite RelA:p50 species **(GR-5)**	**excluded**; Justification for exclusion is similar to GR-1.
6	➔tIkBa (Induced by	4.00E-07 $nM^{-2}.min^{-1}$	NF-κB induced	**included**; GR-6 represent signal

	RelA:p50)		synthesis of *Nfkbia* mRNA encoding IκBα (**GR-6**)	responsiveness of the *Nfkbia* promoter. NF-κB induced expression of a given target gene exhibits variability in different cell-types owing to differences in the chromatin regulations, such as acetylation, methylation etc (*19*). Given the chromatin effects associated with a given promoter is rather independent of the identity of the NF-κB dimers, RelA:p50 and RelA:p52 mediated transcriptional synthesis rate constants were grouped together.
10	➔tIkBa(Induced by RelA:p52)	4.00E-07 $nM^{-2}.min^{-1}$		
7	➔tIkBb (Induced by RelA:p50)	1.20E-08 $nM^{-2}.min^{-1}$	NF-κB induced synthesis of *Nfkbib* mRNA encoding IκBβ (**GR-7**)	**included**; GR-7 represent signal responsiveness of the *Nfkbib* promoter, justification for grouping and inclusion is similar to GR-6.
11	➔tIkBb(Induced by RelA:p52)	1.20E-08 $nM^{-2}.min^{-1}$		
8	➔tIkBe(Induced by RelA:p50)	5.00E-09 $nM^{-2}.min^{-1}$	NF-κB induced synthesis of *Nfkbie* mRNA encoding IκBε (**GR-8**)	**included**; GR-8 represent signal responsiveness of the *Nfkbie* promoter, justification for grouping and inclusion is similar to GR-6.
12	➔tIkBe(Induced by RelA:p52)	5.00E-09 $nM^{-2}.min^{-1}$		
9	➔tp100(Induced by RelA:p50)	2.00E-08 $nM^{-2}.min^{-1}$	NF-κB induced synthesis of *Nfkb2* mRNA encoding p100 (**GR-9**)	**included**; GR-9 represent signal responsiveness of the *Nfkb2* promoter, justification for grouping and inclusion is similar to GR-6.
13	➔tp100(Induced by RelA:p52)	2.00E-08 $nM^{-2}.min^{-1}$		
14	tIkBa ➔	3.50E-02 min^{-1}	constitutive degradation of *Nfkbia* mRNA (**GR-10**)	**excluded**; GR-10 represent signal independent degradation of *Nfkbia* mRNA, which depends on the genetic sequence of the mRNA, and expected to be invariant in different cell-types.
15	tIkBb ➔	3.00E-03	constitutive degradation of *Nfkbib*	**excluded**; Justification for exclusion is similar

		min^{-1}	mRNA (**GR-11**)	to GR-10.
16	tIkBe ➔	4.00E-03 min^{-1}	constitutive degradation of *Nfkbie* mRNA (**GR-12**)	**excluded**; Justification for exclusion is similar to GR-10.
17	tp100 ➔	1.60E-03 min^{-1}	constitutive degradation of *Nfkb2* mRNA (**GR-13**)	**excluded**; Justification for exclusion is similar to GR-10.
18	tNFkB1 ➔	1.00E-03 min^{-1}	constitutive degradation of mRNA encoding RelA:p50 species (**GR-14**)	**excluded**; Justification for exclusion is similar to GR-10.
19	➔IkBa	1.00E+00 min^{-1}	translational synthesis of IκBα (**GR-15**).	**included**; GR-15 represent constitutive synthesis of IκBα proteins from *Nfkbia* mRNAs. A recent study by Kristensen et. al., (*22*) have demonstrated that protein synthesis rate varies considerably among different cell types. Hence these groups were included in global sensitivity analysis.
20	➔IkBb	1.00E+00 min^{-1}	translational synthesis of IκBβ (**GR-16**).	**included**; justification for inclusion is similar to GR-15.
21	➔IkBe	1.00E+00 min^{-1}	translational synthesis of IκBε (**GR-17**).	**included**; justification for inclusion is similar to GR-15.
22	➔p100	5.00E-01 min^{-1}	translational synthesis of p100/*Nfkb2*(**GR-18**).	**included**; justification for inclusion is similar to GR-15.
23	➔RelA:p50	1.00E+00 min^{-1}	translational synthesis of RelA:p50 species in the model (**GR-19**).	**included**; GR-19 represents the composite reaction depicting the production of RelA:p50 dimers in our mathematical model. With a similar justification as that of GR-15, we

				included this group in the global sensitivity analysis.
24	IkBa ➔	1.38E-01 min^{-1}	signal independent, constitutive degradation of IκBα in its free or NF-κB bound form in the cytoplasm and nucleus (**GR-20**)	**excluded**; GR-20 represents signal-independent, constitutive degradation of IκBα either in its free form or in NF-κB complexes. Constitutive degradation rates are different for free and NF-κB-bound IκBα. A change in the rate of degradation for bound IκBα is likely to impact the free protein degradation rate. Accordingly, they were grouped together. As discussed, Kristensen et. al., (*22*) have demonstrated that constitutive protein degradation rates are unlikely to vary among different cell-types. So this parameter group was excluded.
63	IkBa:RelA:p50➔ RelA:p50	6.00E-05 min^{-1}		
67	IkBa:RelA:p52➔ RelA:p52	6.00E-05 min^{-1}		
25	IkBb ➔	2.07E-01 min^{-1}	signal independent, constitutive degradation of IκBβ in its free or NF-κB bound form in the cytoplasm and nucleus (**GR-21**)	**excluded**; justification for grouping and exclusion is similar to GR-20.
64	IkBb:RelA:p50➔ RelA:p50	6.00E-05 min^{-1}		
68	IkBb:RelA:p52 ➔ RelA:p52	6.00E-05 min^{-1}		
26	IkBe ➔	1.73E-01 min^{-1}	signal independent, constitutive degradation of IκBε in its free or NF-κB bound form in the cytoplasm and nucleus (**GR-22**)	**excluded**; justification for grouping and exclusion is similar to GR-20.
65	IkBe:RelA:p50➔ RelA:p50	6.00E-05 min^{-1}		
69	IkBe:RelA:p52➔ RelA:p52	6.00E-05 min^{-1}		
27	IkBd ➔	2.40E-04 min^{-1}	signal independent,	**excluded**; justification for grouping and

66	IkBd:RelA:p50➔ RelA:p50	6.00E-05 min^{-1}	constitutive degradation of IκBδ in its free or NF-κB bound form in the cytoplasm and nucleus (**GR-23**)	exclusion is similar to GR-20.
70	IkBd:RelA:p52➔ RelA:p52	6.00E-05 min^{-1}		
28	p100 ➔	4.00E-01 min^{-1}	signal independent, constitutive degradation of unbound p100 in the cytoplasm and nucleus (**GR-24**)	**excluded**; justification for grouping and exclusion is similar to GR-20.
29	RelA:p50 ➔	2.40E-04 min^{-1}	signal independent, constitutive degradation of RelA:p50 dimer in its free or IκB bound form, in the cytoplasm and nucleus (**GR-25**)	**excluded**; GR-25 represents signal-independent, constitutive degradation of RelA:p50 either in its free form or in IκB bound complexes. Justification for grouping and exclusion is similar to GR-20.
71	IkBa:RelA:p50➔ IkBa	6.00E-05 min^{-1}		
72	IkBb:RelA:p50➔ IkBb	6.00E-05 min^{-1}		
73	IkBe:RelA:p50➔ IkBe	6.00E-05 min^{-1}		
74	IkBd:RelA:p50➔ IkBd	6.00E-05 min^{-1}		
30	RelA:p52 ➔	2.40E-04 min^{-1}	signal independent, constitutive degradation of RelA:p52 dimer in its free or IκB bound form, in the cytoplasm and nucleus (**GR-26**)	**excluded**; GR-26 represents signal-independent, constitutive degradation of RelA:p52 either in its free form or in IκB bound complexes. Justification for grouping and exclusion is similar to GR-20.
75	IkBa:RelA:p52➔ IkBa	6.00E-05 min^{-1}		
76	IkBb:RelA:p52➔ IkBb	6.00E-05 min^{-1}		
77	IkBe:RelA:p52➔ IkBe	6.00E-05 min^{-1}		

78	IkBd:RelA:p52➔ IkBd	6.00E-05 min^{-1}		
103	p100+p100➔IkBd	8.10E-02 $nM^{-1}.min^{-1}$	p100 homo-oligomerization reaction (**GR-27**)	**excluded**; Fundamental biophysical characteristics intrinsic to p100 determine its oligomerization rate and this parameter is unlikely to change in different cell-types (*19*).
47	RelA:p50 + IkBa ➔ IkBa:RelA:p50	3.00E-02 $nM^{-1}.min^{-1}$	association between RelA NF-κB dimers and IκBα in the cytoplasm and nucleus (**GR-28**)	**excluded**; Fundamental biophysical characteristics intrinsic to the interacting molecules determine their association rate parameters and these parameters are unlikely to change in different cell-types (*19*).
51	RelA:p52 + IkBa ➔IkBa:RelA:p52	1.50E-03 $nM^{-1}.min^{-1}$		
48	RelA:p50 + IkBb ➔ IkBb:RelA:p50	3.00E-02 $nM^{-1}.min^{-1}$	association between RelA NF-κB dimers and IκBβ in the cytoplasm and nucleus (**GR-29**)	**excluded**; Justification for grouping and exclusion is similar to GR-28.
52	RelA:p52 + IkBb ➔IkBb:RelA:p52	1.50E-03 $nM^{-1}.min^{-1}$		
49	RelA:p50 + IkBe ➔ IkBe:RelA:p50	3.00E-02 $nM^{-1}.min^{-1}$	association between RelA NF-κB dimers and IκBε in the cytoplasm and nucleus (**GR-30**)	**excluded**; Justification for grouping and exclusion is similar to GR-28.
53	RelA:p52 + IkBe ➔IkBe:RelA:p52	1.50E-03 $nM^{-1}.min^{-1}$		
50	RelA:p50 + IkBd ➔ IkBd:RelA:p50	3.00E-02 $nM^{-1}.min^{-1}$	association between RelA NF-κB dimers and IκBδ in the cytoplasm and nucleus (**GR-31**)	**excluded**; Justification for grouping and exclusion is similar to GR-28.
54	RelA:p52 + IkBd ➔IkBd:RelA:p52	1.50E-03 $nM^{-1}.min^{-1}$		

104	IkBd➔p100+p100	1.20E-05 min^{-1}	dissociation of IκBδ/p100 homo-oligomer (**GR-32**)	**excluded**; Fundamental biophysical characteristics intrinsic to p100 determine the dissociation rate of p100 oligomer and this parameter is unlikely to change in different cell-types (*19*).
55	IkBa:RelA:p50 ➔RelA:p50 + IkBa	6.00E-05 min^{-1}	dissociation of the complex composed of RelA NF-κB dimers and IκBα in the cytoplasm and nucleus (**GR-33**)	**excluded**; GR-33 represents dissociation rates of NF-κB-IκBα complexes. Fundamental biophysical characteristics of the interacting molecules determine these rate parameters and these parameters are unlikely to change in different cell-types (*19*).
59	IkBa:RelA:p52 ➔RelA:p52 + IkBa	6.00E-05 min^{-1}		
56	IkBb:RelA:p50 ➔RelA:p50 + IkBb	6.00E-05 min^{-1}	dissociation of the complex composed of RelA NF-κB dimers and IκBβ in the cytoplasm and nucleus (**GR-34**)	**excluded**; Justification for grouping and exclusion is similar to GR-33.
60	IkBb:RelA:p52 ➔RelA:p52 + IkBb	6.00E-05 min^{-1}		
57	IkBe:RelA:p50 ➔RelA:p50 + IkBe	6.00E-05 min^{-1}	dissociation of the complex composed of RelA NF-κB dimers and IκBε in the cytoplasm and nucleus (**GR-35**)	**excluded**; Justification for grouping and exclusion is similar to GR-33.
61	IkBe:RelA:p52 ➔RelA:p52 + IkBe	6.00E-05 min^{-1}		
58	IkBd:RelA:p50 ➔RelA:p50 + IkBd	6.00E-05 min^{-1}	dissociation of the complex composed of RelA NF-κB dimers and IκBδ in the cytoplasm and nucleus (**GR-36**)	**excluded**; Justification for grouping and exclusion is similar to GR-33.
60	IkBd:RelA:p52 ➔RelA:p52 + IkBd	6.00E-05 min^{-1}		
31	IkBa + NEMO-	1.95E-03 $nM^{-1}.min^{-1}$	NEMO-IKK2	**included**; GR-37 represents IKK2 mediated

	IKK2➔		mediated degradation of free or RelA:p50 or RelA:p52 bound IκBα in the cytoplasm. (**GR-37**)	degradation of IκBα in its free or NF-κB bound form. Quantitative as well as qualitative variations in receptor and adapter complexes in different cell-types impart changes in the signal strength (*19*), which is expected to alter IKK2 mediated degradation rates. As such, the variation in IKK2 mediated degradation rate of a given IκB species is independent of the complex in which the IκB species belongs. Accordingly, all three IKK2 mediated IκBα degradation rates were grouped together.
79	NEMO-IKK2 +IkBa:RelA:p50 ➔RelA:p50	1.95E-03 $nM^{-1}.min^{-1}$		
82	NEMOIKK2 +IkBa:RelA:p52 ➔RelA:p52	1.95E-03 $nM^{-1}.min^{-1}$		
32	IkBb + NEMO-IKK2➔	5.00E-04 $nM^{-1}.min^{-1}$	NEMO-IKK2 mediated degradation of free or RelA:p50 or RelA:p52 bound IκBβ in the cytoplasm. (**GR-38**)	**included**; GR-38 represents IKK2 mediated degradation of IκBβ in its free or NF-κB bound form, justification for grouping and inclusion is similar to GR-37.
80	NEMO-IKK2 +IkBb:RelA:p50 ➔RelA:p50	5.00E-04 $nM^{-1}.min^{-1}$		
83	NEMO-IKK2+ IkBb:RelA:p52 ➔RelA:p52	5.00E-04 $nM^{-1}.min^{-1}$		
33	IkBe + NEMO-IKK2➔	5.00E-04 $nM^{-1}.min^{-1}$	NEMO-IKK2 mediated degradation of free or RelA:p50 or RelA:p52 bound IκBε in the cytoplasm. (**GR-39**)	**included**; GR-39 represents IKK2 mediated degradation of IκBε in its free or NF-κB bound form, justification for grouping and inclusion is similar to GR-37.
81	NEMO-IKK2 +IkBe:RelA:p50 ➔RelA:p50	5.00E-04 $nM^{-1}.min^{-1}$		
84	NEMO-IKK2+ IkBe:RelA:p52 ➔RelA:p52	5.00E-04 $nM^{-1}.min^{-1}$		
34	IkBd+NIK-IKK1➔	1.00E-03 $nM^{-1}.min^{-1}$	NIK-IKK1 mediated degradation of free or RelA:p50 or RelA:p52	**included**; GR-40 represents NIK-IKK1 mediated degradation of IκBδ in its free or NF-
85	NIK-IKK1	1.00E-03 $nM^{-1}.min^{-1}$		

	+IkBd:RelA:p50 ➔RelA:p50		bound IκBδ in the cytoplasm. (**GR-40**)	κB bound form. Quantitative as well as qualitative variations in receptor and adapter complexes in different cell-types impart changes in the signal strength (*19*), which is expected to be reflected in NIK-IKK1 mediated degradation rates. As such, the variation in NIK-IKK1 mediated degradation rate of IκBδ is independent of the complex in which IκBδ belongs. Accordingly, all three NIK-IKK1 mediated IκBδ degradation rates were grouped together.
86	NIK-IKK1 +IkBd:RelA:p52 ➔ RelA:p52	1.00E-03 $nM^{-1}.min^{-1}$		
105	NIK-IKK1 +p100➔RelA:p52	4.20E-03 $nM^{-1}.min^{-1}$	NIK-IKK1 mediated RelA:p52 generation from p100 (**GR-41**)	**included**; GR-41 represents NIK-IKK1 mediated generation of RelA:p52 dimer from p100. Justification for inclusion is similar to GR-40.
35	IkBa ➔IkBan	9.00E-02 min^{-1}	nuclear import of free IκBs or RelA NF-κB dimers or IκB-NF-κB complexes (**GR-42**)	**excluded**; GR-42 represents nuclear import of various NF-κB/IκB species. Cell-type specific changes in the abundance and biochemical composition of nuclear pores has been observed (*49*). These variations are expected to affect nuclear import rates (grouped together) of various NF-κB/IκB complexes similarly. However, prior modeling analyses confirmed that these parameters are not rate limiting (*19*) and therefore were excluded from the global sensitivity analysis.
36	IkBb ➔IkBbn	9.00E-03 min^{-1}		
37	IkBe ➔IkBen	4.50E-02 min^{-1}		
38	IkBd ➔IkBdn	4.50E-02 min^{-1}		
39	RelA:p50 ➔ RelA:p50n	5.40E+00 min^{-1}		
87	IkBa:RelA:p50➔ IkBa:RelA:p50n	2.70E-01 min^{-1}		
88	IkBb:RelA:p50➔ IkBb:RelA:p50n	2.70E-02 min^{-1}		
89	IkBe:RelA:p50➔ IkBe:RelA:p50n	1.30E-01 min^{-1}		
90	IkBd:RelA:p50➔	2.70E-01 min^{-1}		

	IkBd:RelA:p50n			
40	RelA:p52 ➔ RelA:p52n	5.40E+00 min^{-1}		
91	IkBa:RelA:p52➔ IkBa:RelA:p52n	2.70E-01 min^{-1}		
92	IkBb:RelA:p52➔ IkBb:RelA:p52n	2.70E-02 min^{-1}		
93	IkBe:RelA:p52➔ IkBe:RelA:p52n	1.30E-01 min^{-1}		
94	IkBd:RelA:p52➔ IkBd:RelA:p52n	2.70E-01 min^{-1}		
41	IkBan ➔IkBa	1.20E-02 min^{-1}	nuclear export of free IκBs or RelA NF-κB dimers or IκB-NF-κB complexes (**GR-43**)	**excluded**; GR-43 represents nuclear export of various NF-κB/IκB species, justification for grouping and inclusion is similar to GR-42.
42	IkBbn ➔IkBb	1.20E-02 min^{-1}		
43	IkBen ➔IkBe	1.20E-02 min^{-1}		
44	IkBdn ➔IkBd	1.20E-02 min^{-1}		
45	RelA:p50n ➔RelA:p50	1.80E-03 min^{-1}		
95	IkBa:RelA:p50n➔ IkBa:RelA:p50	8.30E-01 min^{-1}		
96	IkBb:RelA:p50n➔ IkBb:RelA:p50	4.10E-01 min^{-1}		
97	IkBe:RelA:p50n➔ IkBe:RelA:p50	4.10E-01 min^{-1}		
98	IkBd:RelA:p50n➔ IkBd:RelA:p50	4.10E-01 min^{-1}		

46	RelA:p52n ➔ RelA:p52	1.80E-03 min^{-1}		
99	IkBa:RelA:p52n➔ IkBa:RelA:p52	8.30E-01 min^{-1}		
100	IkBb:RelA:p52n➔ IkBb:RelA:p52	4.10E-01 min^{-1}		
101	IkBe:RelA:p52n➔ IkBe:RelA:p52	4.10E-01 min^{-1}		
102	IkBd:RelA:p52n➔ IkB2:RelA:p52	4.10E-01 min^{-1}		

Table S2. List of notations used in the model to describe different biochemical species.

Model species	Nomenclature	Location
IkBα	IkBa	cytoplasm
IkBαn	IkBan	nucleus
Nfkbia mRNA	tIkBa	cytoplasm
IkBβ	IkBb	cytoplasm
IkBβn	IkBbn	nucleus
Nfkbib mRNA	tIkBb	cytoplasm
IkBε	IkBe	cytoplasm
IkBεn	IkBen	nucleus
Nfkbie mRNA	tIkBe	cytoplasm
IkBδ	IkBd	cytoplasm
IkBδn	IkBdn	nucleus
p100	p100	cytoplasm
Nfkb2 mRNA	tp100	cytoplasm
RelA:p50	RelA:p50	cytoplasm
RelA:p50n	RelA:p50n	nucleus
NFkB1 mRNA	tNFkB1	cytoplasm
RelA:p52	RelA:p52	cytoplasm
RelA:p52n	RelA:p52n	nucleus
IkBα:RelA:p50	IkBaN:RelA:p50	cytoplasm
IkBα:RelA:p50n	IkBa:RelA:p50n	nucleus
IkBβ: RelA:p50	IkBb:RelA:p50	cytoplasm
IkBβ:RelA:p50n	IkBb:RelA:p50n	nucleus
IkBε:RelA:p50	IkBe:RelA:p50	cytoplasm
IkBε:RelA:p50n	IkBe:RelA:p50n	nucleus
IkBδ:RelA:p50	IkBd:RelA:p50	cytoplasm
IkBδ:RelA:p50n	IkBd:RelA:p50n	nucleus
IkBα:RelA:p52	IkBa:RelA:p52	cytoplasm
IkBα:RelA:p52n	IkBa:RelA:p52n	nucleus
IkBβ:RelA:p52	IkBb:RelA:p52	cytoplasm
IkBβ:RelA:p52n	IkBb:RelA:p52n	nucleus
IkBε:RelA:p52	IkBe:RelA:p52	cytoplasm
IkBε:RelA:p52n	IkBe:RelA:p52n	nucleus
IkBδ:RelA:p52	IkBd:RelA:p52	cytoplasm
IkBδ:RelA:p52n	IkBd:RelA:p52n	nucleus
NEMO-IKK2	NEMO-IKK2	cytoplasm
NIK-IKK1	NIK-IKK1	cytoplasm